Factors affecting the Faradaic efficiency of Fe(0) electrocoagulation

CrossMark

C.M. van Genuchten[a,b,*], K.N. Dalby[b], M. Ceccato[b], S.L.S. Stipp[b], K. Dideriksen[b]

[a] Department of Earth Sciences-Geochemistry, Faculty of Geosciences, Utrecht University, Utrecht 3508TA, The Netherlands
[b] Nano-Science Center, Department of Chemistry, University of Copenhagen, Copenhagen, Denmark

ARTICLE INFO

ABSTRACT

Electrocoagulation (EC) using Fe(0) electrodes is a low cost water treatment technology that relies on efficient production of Fe(II) from the electrolytic dissolution of Fe(0) electrodes (i.e. a high Faradaic efficiency). However, the (electro)chemical factors that favor Fe(0) oxidation rather than O$_2$ evolution during Fe(0) EC have not been identified. In this study, we combined electrochemical methods, electron microscopy and Fe measurements to systematically examine the interdependent effects of current density (i), anodic interface potential (E_A) and solution chemistry on the Faradaic efficiency. We found that Fe(0) oxidation was favored (Faradaic efficiency > 0.85) in chloride and bromide solutions at all i, whereas carbonate, phosphate, citrate, and nitrate solutions lead to Faradaic efficiencies < 0.1. The anodic reaction (i.e. Fe(0) oxidation or O$_2$ evolution) only depended on i in the sulfate and formate solutions. Experiments in binary-anion solutions revealed that molar ratios of $[HCO_3^-]/[Cl^-]$ near 100 and $[NO_3^-]/[Cl^-]$ near 20 separated the electrochemical domains of Fe(0) oxidation and O$_2$ evolution in the EC system. These molar ratios were supported by experiments in synthetic groundwater solutions. We also found that the E_A vs i curves for solutions with poor Faradaic efficiency overlapped but were situated 2–4 V vs Ag/AgCl higher than those of solutions with high Faradaic efficiency. Therefore, the position of the E_A vs i curve, rather than the E_A alone, can be used to determine unambiguously the reaction occurring on the Fe(0) anode during EC treatment.

1. Introduction

Electrocoagulation (EC) using Fe(0) electrodes is a promising, low cost treatment technology for drinking water and wastewater. This technology is particularly applicable in decentralized and rural areas because of its low infrastructure requirements, ease of use and potential for scalability [1,2]. While EC systems are often accompanied by supplementary treatment steps, including settling tanks and filters [3], the technology centers on applying an electric current to Fe(0) electrodes in contact with an electrolyte solution to promote the oxidative release of soluble Fe(II) ions [4,5]. The Fe(II) ions migrate from the Fe(0) anode surface to the bulk solution, where contaminant removal occurs by several possible pathways. For example, Fe(II) ions can immobilize target species through direct reduction reactions (e.g. chromate) [6–9] or they can be oxidized by dissolved oxygen and Fenton-type intermediates (e.g. $^*O_2^-$, H_2O_2, and Fe(IV) or $^*OH$ [10,11]) to produce reactive Fe(III) (oxyhydr)oxides that remove contaminants by sorption (e.g. arsenic [12,13], heavy metals [14], dyes [15,16], perfluoroalkyl acids [17], and pathogens [18]). In addition, the oxidized Fe(II) ions

form solid flocs that can be used as a pre-treatment step for additional purification processes, such as membrane filtration or advanced oxidation [19,20]. In recent years, the molecular scale mechanisms of contaminant removal in the bulk solution during Fe(0) EC treatment have been the focus of considerable research [19,21–23]. However, few EC studies have examined the electron transfer reactions occurring at the Fe(0) anode [24,25], which are responsible for the production of Fe(II). Because Fe(0) EC treatment relies on the production of Fe(II) from the Fe(0) anode [26,27], it is essential to understand the factors that promote efficient Fe(II) generation.

In EC, the concentration of Fe(II) (mol/L) generated at the Fe(0) anode is related to the applied current by Faraday's law:
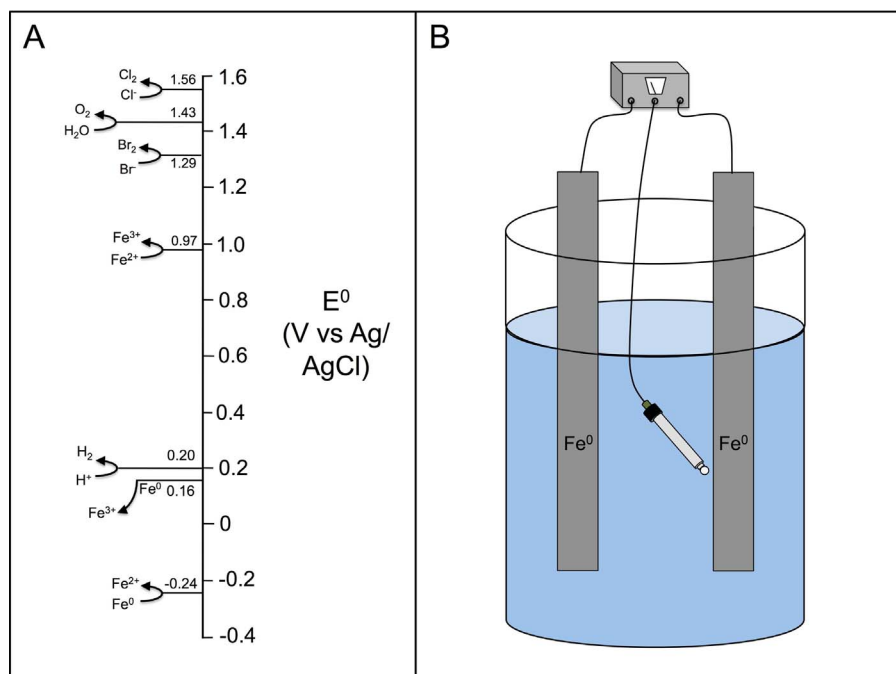
$$[Fe] = (I \cdot t)/(n \cdot F \cdot V) \tag{1}$$

where I represents the current (C/s) applied for time, t (s), n represents the number of electrons transferred ($n = 2$ for Fe(II) production, consistent with previous work [4]), F, the Faraday constant (96,485 C/mol) and V, the solution volume (L). From Eq. (1), we can define the Faradaic efficiency as the Fe concentration measured in the bulk solution,

Fig. 1. A) Standard redox potentials (E^0) for half reactions that can occur on the Fe(0) anode surface during EC. E^0 is reported for standard state conditions in units of V vs Ag/AgCl, which is a +0.2 V difference relative to the standard hydrogen electrode (SHE) [50]. B) Schematic representation of the set up for electrochemical experiments.

normalized by the theoretical Fe(II) concentration calculated by Faraday's law. Therefore, a Faradaic efficiency near 1 indicates the production of Fe(II) and optimum system performance. Conversely, a drop in Faradaic efficiency, and thus treatment efficiency, can occur when the applied current drives the anodic oxidation of H_2O or coexisting solutes, rather than Fe(0). As shown in Fig. 1a, the anodic oxidation of Fe(0) to form Fe(II) occurs at a low standard redox potential (E^0), whereas the oxidation of H_2O, chloride, or bromide can be favored as the anodic interface potential increases above 1.0 V vs Ag/AgCl. Therefore, knowledge of the interface potential, which relates to the thermodynamic driving force of electrode reactions [28], is critical to deconvolute the factors that affect the Faradaic efficiency of Fe(0) EC.

Based on previous research, we can identify a number of (electro) chemical parameters that can potentially influence the Faradaic efficiency and interface potential [24,25,29]. For example, the Butler-Volmer relationship shows that the applied current is directly proportional to the interface potential:

$$i = I/A = i_0 \cdot [(\exp(\alpha_A \cdot E_A) - (\exp(\alpha_C \cdot E_C)] \qquad (2)$$

where i represents the current density (mA/cm²), A, the electrode surface area (cm²), i_0, the exchange current density (mA/cm²), α_A and α_C represent constants (detailed in Supplementary material) and E_A and E_C represent the anode and cathode interface potentials (V). Therefore, an increase in i (or I for a constant electrode surface area) can increase the anodic interface potential (E_A) to levels high enough to yield O_2, Cl_2 or Br_2 (Fig. 1a), which would decrease the Faradaic efficiency. This relationship between i and the Faradaic efficiency in Al(0) and Fe(0) EC studies has been reported for a limited range of electrolyte solutions (e.g. nitrate [30] and sulfate [24,25,29]). However, the absence of E_A measurements in most Fe(0) EC investigations has prevented reliable explanations of the impact of i on the Faradaic efficiency.

Another factor likely to influence the Faradaic efficiency is the ionic composition of the solution. For example, Arroyo et al. (2010) measured a Faradaic efficiency of ~1.0 for Fe(0) EC experiments in a chloride solution [31], whereas a reduced Faradaic efficiency has been reported in sulfate and nitrate solution at circumneutral pH [25,30]. However, these previous Fe(0) EC studies investigated a limited range of i and did not examine the impact of a wide variety of electrolyte solutions. A number of other inorganic and organic ions that are ubiquitous in natural systems, including carbonate, phosphate, formate

and citrate, have been shown to interact with Fe(0) surfaces to inhibit the oxidation of Fe(0) in passive corrosion systems [32,33]. The impact of these environmentally relevant ions on the Faradaic efficiency of Fe (0) EC is poorly constrained, leading to a critical knowledge gap. Because Fe(0) EC treatment for a wide range of influent compositions hinges on maintaining a high Faradaic efficiency and minimizing electrode passivation, it is essential to investigate systematically the relationship between i, E_A and Faradaic efficiency in a diverse set of solution compositions.

In this work, our objective was to determine the (electro)chemical factors that govern the Faradaic efficiency of Fe(0) EC. To this end, we investigated the interdependent effects of i, E_A and solution composition by combining time dependent measurements of E_A and total Fe released from the Fe(0) anode as a function of i and solution chemistry. To encompass the range of current densities likely applied in Fe(0) EC field treatment [3], the i of EC experiments was adjusted over two orders of magnitude (0.25–50 mA/cm²). The impact on the Faradaic efficiency of a variety of dissolved species common in natural waters was studied by systematically varying the ionic composition and pH of the solution, building in complexity from single and binary anion systems to synthetic groundwater matrices. Micrometer scale modifications on the surface of Fe(0) anodes used in the EC experiments were probed by scanning electron microscopy (SEM). Our approach allowed us to elucidate the impact of solution chemistry and EC operating parameters on the redox reactions occurring at the Fe(0) anode, which has not been investigated previously and is critical for predicting and optimizing the performance of Fe(0) EC treatment under a wide range of source water chemistry. The ultimate aim of this study was to identify simple and low cost strategies to improve Fe(0) EC treatment in waters having compositions that result in poor Faradaic efficiency.

2. Materials and methods

2.1. Preparation of the electrolyte solutions

All chemicals used to prepare the stock solutions were reagent grade and all glassware was acid washed and rinsed three times with 18 MΩ·cm Milli-Q deionized (DI) water prior to use. Stock solutions of sodium chloride (NaCl, 0.5 M), potassium bromide (KBr, 0.2 M), sodium sulfate (Na_2SO_4, 0.2 M), sodium bicarbonate ($NaHCO_3$, 0.5 M),

Table 1
Composition, conductivity and E_A ($i = 1$ mA/cm^2) for single anion electrolyte solutions.

Electrolyte	Anion Concentration (mM)	Ionic Strength (M)	Conductivity[a] (dS/m)	E_A at $i = 1$ mA/cm2 (V vs Ag/AgCl)
Chloride	10	0.010	0.79	− 0.1
Bromide	10	0.010	0.79	0.0
Sulfate	5	0.015	1.18	0.1
Carbonate	10	0.010	0.79	1.6
Phosphate	5	0.015	1.18	1.3
Nitrate	10	0.010	0.79	1.6
Formate	10	0.010	0.79	1.4
Citrate	5	0.030	2.36	1.5

[a] Conductivity was determined using the Griffin-Jurinak relation [62].

Table 2
Compositions and conductivity of the synthetic groundwaters.

Electrolyte		SBGW[a]	NO$_3$-GW 1	NO$_3$-GW 2
Ionic Strength		0.046	0.153	0.341
Conductivity[b] (dS/m)		3.53	11.7	26.2
Ionic Composition (mM)	pH	7.5	5.5	3.5
	Ca^{2+}	2.5	5.2	25.1
	Mg^{2+}	1.6	3.5	6.8
	HPO_4^{2-}	0.1	0	0
	SO_4^{2-}	0	15	10
	$[HCO^{3-}]$	8.2	10	0
	NO^{3-}	0	17.3	133
	Cl^-	4.1	0.5	7.3
	$[HCO_3^-]/[Cl]$	2.0	20	0
	$[NO_3^-]/[Cl]$	0	34.6	18.2

[a] SBGW also contained 1.1 mM H_4SiO_4. Sodium is not included in this table but is used to balance electroneutrality. The total bicarbonate is represented by $[HCO_3^-]$. The open circuit potential was − 0.2 V vs Ag/AgCl for all solutions except NO$_3$-GW 2, which had an open circuit potential of − 0.5 V vs Ag/AgCl.

[b] Conductivity was determined using the Griffin-Jurinak relation [62].

sodium phosphate (Na$_2$HPO$_4$, 0.2 M), sodium nitrate (NaNO$_3$, 0.2 M), sodium formate (NaHCOO, 0.2 M) and sodium citrate (Na$_3$C$_3$H$_5$O (COO)$_3$, 0.2 M) were stored in air tight containers at room temperature. Single anion electrolyte solutions were produced by combining stock solutions and air saturated DI water to yield 10 mM concentrations of chloride, bromide, formate, nitrate and carbonate and 5 mM concentrations of sulfate, phosphate and citrate. In a separate group of experiments, we varied the molar ratio of $[NO_3^-]/[Cl^-]$ and $[HCO_3^-]/[Cl^-]$ in binary anion electrolyte solutions by diluting nitrate, carbonate and chloride stock solutions in air saturated DI water. In these experiments, at least one anion was always 10 mM and the other was lowered to yield $[NO_3^-]/[Cl^-]$ or $[HCO_3^-]/[Cl^-]$ molar ratios ranging from 0.1 to 1000. In Table 1, we summarize the composition and conductivity of all single anion electrolyte solutions.

After adding all components to the single or binary anion solutions, the initial pH was set to 7.5 ± 0.5, unless otherwise noted, using small amounts of NaOH or the respective acid of the electrolyte anion (i.e. H$_3$PO$_4$ for phosphate experiments, HNO$_3$ for nitrate experiments, etc). The amount of acid/base added changed the anion concentration by less than 1%. Preliminary electrochemical experiments at pH 7.5 (described below) revealed that pH did not drift substantially (< 0.5 units) during the reaction. In addition to experiments performed at circumneutral pH, we also examined solutions with a range of pH from 4.0 ± 0.5 to 11.0 ± 0.5 for sulfate and phosphate single anion solutions. In these experiments, solution pH drifted to neutral during preliminary EC experiments. Therefore, we added dilute concentrations of H$_2$SO$_4$ and H$_3$PO$_4$ (pH 4 experiments) or NaOH (pH 11 experiments) during electrolysis to minimize pH drift (< 0.5 units). The amount of acid used to decrease pH during experiments increased the anion concentration by < 10%.

In addition to single and binary anion electrolyte solutions, we also prepared a series of synthetic groundwater matrices (Table 2), which were designed to mimic a range of contaminated groundwaters that are candidates for Fe(0) EC field treatment [34–38]. For arsenic contaminated groundwater (pH 7.5), we prepared a synthetic Bangladesh groundwater (SBGW) electrolyte solution following a recipe derived from a British Geological Survey analysis of thousands of groundwater wells in Bangladesh [39]. For groundwater co-contaminated by uranium and nitrate (pH 3.5–5.5), which can occur at sites of uranium enrichment [37], we prepared two nitrate contaminated groundwaters (NO$_3$-GW 1 and NO$_3$-GW 2) that were made to mimic the composition of contaminated groundwaters reported previously [40–44]. Because of their trace concentrations, arsenic and uranium were excluded from the synthetic groundwater recipes.

2.2. Electrochemical experiments

Electrochemical experiments were performed with a Metrohm-Autolab potentiostat (Utrecht, the Netherlands) operated in a three electrode system (Fig. 1b). The electrochemical cell consisted of an Ag/

AgCl reference electrode and Fe(0) working and counter electrodes (spaced 2 cm apart). The trace metal composition of the Fe(0) electrodes used in our study was reported previously [45]. Before each experiment, the Fe(0) electrodes were cleaned and polished with fine grained sandpaper. Because a positive electrochemical potential was applied to the working electrode in each of our experiments, we refer to the Fe(0) working electrode as the anode and the Fe(0) counter electrode as the cathode in this work. Experiments were initiated by applying a galvanostatic current to the electrochemical cell with the electrolyte solution mixed by a magnetic stir bar. Experiments were performed open to the atmosphere, which allows for CO$_{2(g)}$ dissolution but equilibrium speciation calculations predict a maximum of ~0.1 mM HCO$_3^-$ and 1 μM CO$_3^{2-}$ in typical electrolyte solutions, which would not significantly affect the results. Furthermore, the EC experiments are so short that only slight CO$_{2(g)}$ dissolution is expected. The i (0.25–50 mA/cm^2) was set by modifying the applied current (2–400 mA) while maintaining the active surface area of the Fe(0) anode at 8 cm^2. The potentiostat was operated in chronoamperometric mode, with measurements of E_A occurring with 1 s resolution. In typical experiments, we applied a total charge dosage of 40 C/L to a 200 mL electrolyte solution (0.2 mM Fe(II) by Eq. (1)), which corresponds to total electrolysis times of ~0.5 to 20 min. To avoid long electrolysis times however, the solution volume was reduced to 125 mL for experiments with $i \leq 1$ mA/cm^2 and the charge dosage was 20 C/L for experiments at $i \leq 0.5$ mA/cm^2.

At various time steps along the reaction, aliquots of the suspension were removed using a wide mouthed pipette and immediately acidified in 4% HNO$_3$ for analysis of total Fe by atomic absorption spectrometry (AAS, Perkin Elmer AAnalyst 800) at a wavelength of 248.3 nm. Although our measurements of total Fe do not discriminate between Fe (II) and Fe(III), the calculation of Faradaic efficiency does not rely on direct measurements of Fe(II) because the total Fe concentration generated by EC is directly related to the number of electrons transferred between the Fe(0) electrode and the dissolved Fe species (i.e. n = 2 for Fe(II) and n = 3 for Fe(III)). Therefore, if Fe(III) were the dominant species generated, the Faradaic efficiency would be 33% lower than that obtained if Fe(II) is produced. In addition, for experiments at the largest i, chemical dissolution of Fe(0) should not contribute significantly to the Faradaic efficiency because of the rapid time scales of these experiments (< 1 min) [46]. For each data point, the Faradaic efficiency was determined by normalizing the experimental Fe concentration (Fe$_{exp}$, mg/L) measured with AAS by the theoretical Fe concentration (Fe$_{th}$, mg/L) calculated from Eq. (1), assuming the production of Fe(II). In our study, a Faradaic efficiency (Fe$_{exp}$/Fe$_{th}$) of 0 indicates that all charge that passed through the EC cell went to reactions other than Fe(0) oxidation, whereas a Faradaic efficiency of 1 is

consistent with the electrochemical production of only Fe(II). Our results are plotted as the average and standard deviation, where applicable, of replicated experiments, but we note that the variation for many data points (experiments with Faradaic efficiency < 0.1 and most interface potential measurements) was smaller than the size of the plotted data point.

2.3. Scanning electron microscopy with energy dispersive X-ray spectroscopy

Scanning electron microscopy (SEM) and energy dispersive X-ray spectroscopy (EDXS) were used to track surface modifications of the Fe(0) anodes caused by electrolysis. Iron anode samples used in four different electrolyte solutions were prepared by performing 10 of the previously described EC experiments over 3 d in each of the chloride, bromide, nitrate, and citrate solutions. Anodes were rinsed briefly with DI water after each EC experiment and were air dried overnight, which is similar to the operation and drying cycles of electrodes during long term Fe(0) EC field treatment [3]. The surface morphology (SEM) and chemical composition (EDXS) of the Fe(0) anodes were examined before electrolysis (0 runs, cleaned and polished) and after 2 runs (1 d), 6 runs (2 d) and 10 runs (3 d). SEM images were collected with a FEI Quanta 3D FEG SEM equipped with a voltage contrast detector. EDXS spectra were obtained using an Oxford X-Max 20 mm^2 EDXS spectrometer. An accelerating voltage of 20 kV and a current of 8 nA were used during data collection. A conductive coating was not used on the Fe(0) anodes.

3. Results

3.1. Time dependent Fe concentration and anodic interface potential

In Fig. 2, we present an overview of representative data obtained in each electrochemical experiment (i = 1 mA/cm^2) for three electrolyte solutions: chloride, sulfate and nitrate. The Fe generated (Fe$_{exp}$) in both the chloride and sulfate solutions follows closely the theoretical value (Fe$_{th}$) for the production of Fe(II), which is highlighted by one of the shaded regions in Fig. 2a. A subtle trend in the production of Fe with time is also observed for these two electrolytes, with slightly decreased Fe$_{exp}$ values relative to Fe$_{th}$ assuming the constant production of Fe(II) (Eq. (1)). Nevertheless, the Fe$_{exp}$ in the chloride and sulfate electrolyte solutions generally increased linearly with time and a Faradaic efficiency > 0.85 was obtained at all time steps. By contrast, the Fe$_{exp}$ in the nitrate solution was negligible, yielding a Faradaic efficiency < 0.1 throughout electrolysis.

The time dependent anodic interface potential (E_A) measurements for the three electrolyte solutions are shown in Fig. 2b. The E_A in the nitrate solution was substantially higher (1.6 V vs Ag/AgCl) than that measured in the chloride or sulfate solutions (< 0.5 V vs Ag/AgCl), which is consistent with the differences in time dependent Fe$_{exp}$. For the chloride and sulfate solutions, the E_A at i = 1 mA/cm^2 never increased above the E for O$_2$ or Cl$_2$ production (E ≈ 1.02 V vs Ag/AgCl for O$_2$ at pH 7; E ≈ 1.68 V vs Ag/AgCl for Cl$_2$ at 10 mM chloride). This result indicates that significant anodic production of O$_2$ and Cl$_2$ was unlikely. Although the E_A in the sulfate solution decreased slightly over time, it was relatively stable in the chloride and sulfate solutions after the onset of electrolysis. There were no rapid fluctuations to indicate a change in the dominant anodic redox reaction.

Analogous time dependent measurements of Fe$_{exp}$ and E_A were obtained for every electrochemical experiment in our study. However, to simplify the presentation of our results, we note that each data point presented in subsequent figures corresponds to the Faradaic efficiency at the end of electrolysis (i.e. the final time step in Fig. 2a) and E_A measured at the midpoint of electrolysis.
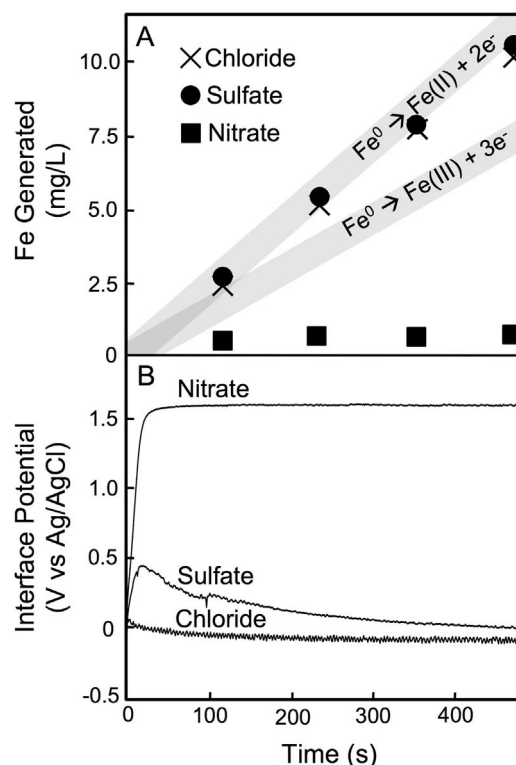

Fig. 2. Measurements of (A) Fe in the bulk electrolyte solution and (B) the anodic interface potential as a function of time for selected solution compositions: 10 mM chloride (crosses), 5 mM sulfate (circles), and 10 mM nitrate (squares). The i was 1 mA/cm^2 and the initial pH was 7.5. The shaded regions in (A) show the hypothetical Faradaic Fe concentrations, assuming the production of Fe(II) and Fe(III).

3.2. Influence of solution composition

3.2.1. Chloride, bromide and sulfate

The Faradaic efficiencies (top panels) and E_A (bottom panels) are plotted as a function of a wide range of i (0.25–50 mA/cm^2) for 8 different inorganic and organic single anion solutions in Fig. 3. The Faradaic efficiencies for the chloride and bromide electrolytes were largely independent of i, with values > 0.8 observed at all i (Fig. 3a). Coinciding with these high Faradaic efficiencies, the Fe(0) anode surfaces after electrolysis in both chloride and bromide solutions developed macroscopic surface modifications that were low in contrast on SEM images, consistent with the formation of less electron dense Fe (oxyhydr)oxide corrosion layers (Fig. 4 and Figs. S1 and S2 in the Supplementary material). By contrast, the Faradaic efficiency in the sulfate solution was strongly dependent on i. At i < 3 mA/cm^2, the Faradaic efficiency was > 0.9, which was similar to that for the bromide and chloride solutions. However, at i ≥ 3 mA/cm^2, the Faradaic efficiency decreased to < 0.1, which indicates that Fe(II) generation was not the dominant anodic reaction.

The shape and position of the E_A vs i curves for the chloride and bromide solutions matched closely (Fig. 3b), which is consistent with their similar Faradaic efficiencies. On a log scale, the E_A increased exponentially from −0.1 to > 5.0 V vs Ag/AgCl with increases in i for both the chloride and bromide solutions. However, there was a linear relationship between E_A and i when i was plotted on a linear scale (Fig. S3). Despite the high Faradaic efficiencies in the chloride and bromide solutions, the E_A at i > 20 mA/cm^2 exceeded the standard state E^0 for the O$_2$/H$_2$O, Cl$_2$/Cl$^-$, and Br$_2$/Br$^-$ redox couples. Although experiments at high i yielded E_A well above the potential required for evolution of Cl$_2$ (E ≈ 1.68 V vs Ag/AgCl), Br$_2$ (E ≈ 1.41 V vs Ag/AgCl) and O$_2$ (E ≈ 1.02 V vs Ag/AgCl), a high Faradaic efficiency was measured and no bubble production was observed. These results indicate that E_A
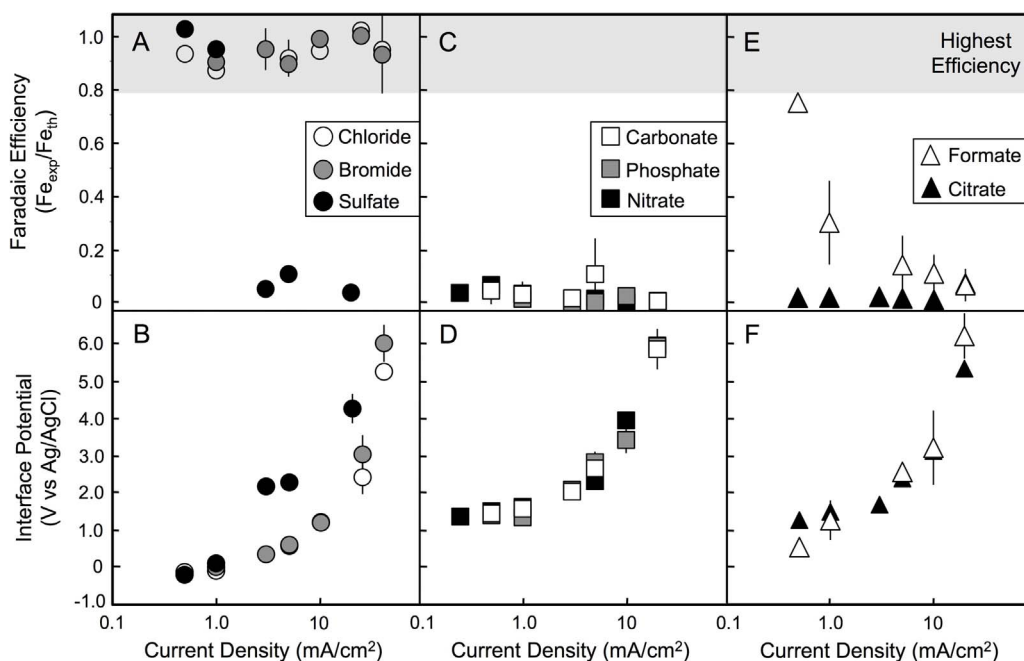
Fig. 3. Faradaic efficiency (top panels) and interface potential (bottom panels) as a function of i for single anion electrolyte solutions. In A) and B), the solutions consisted of 10 mM chloride (open circles), 10 mM bromide (grey circles) and 5 mM sulfate (black circles). In C) and D), the solutions contained 10 mM carbonate (open squares), 5 mM phosphate (grey circles) and 10 mM nitrate (black squares). In E) and F), the solutions consisted of 10 mM formate (open triangles) and 5 mM citrate (black triangles). For all solutions, pH was 7.5.

levels above 5.0 V vs Ag/AgCl do not necessarily entail significant O_2 evolution or chloride/bromide oxidation in these solutions.

Consistent with the distinct i-dependence of the Faradaic efficiency observed in the sulfate solution, the E_A vs i curve for sulfate differs relative to that of chloride and bromide. At $i < 3$ mA/cm^2, the E_A vs i curve for sulfate follows that of chloride and bromide. However, a nonlinear jump in E_A occurs at $i > 3$ mA/cm^2, leading to a ~2 V vs Ag/AgCl increase in E_A relative to that of chloride and bromide electrolyte solutions for $i > 3$ mA/cm^2. Notably, this abrupt increase in E_A coincided with the dramatic decrease in the Faradaic efficiency observed in the same i-range. This indicates the existence of a threshold i in the sulfate solution that delineates the electrochemical domain of Fe (0) oxidation.

3.2.2. Carbonate, phosphate and nitrate

In contrast to the chloride and bromide solutions, poor Faradaic efficiencies were observed in the carbonate, phosphate and nitrate solutions, regardless of i (Fig. 3c). Even for experiments performed at the lowest i, which should lead to the lowest E_A based on Eq. (2), the Faradaic efficiency never exceeded 0.1 for these single anion solutions. In addition, the Fe(0) anode showed no evidence for any Fe (oxyhydr) oxide corrosion layers after 10 runs in the nitrate electrolyte (Fig. 4, Figs. S1 and S2). This observation contrasts with the behavior of the chloride and bromide solutions and is consistent with the passivation of the anode surface [32,33]. Because the ionic strength of the nitrate and halide ion electrolytes was identical (Table 1), these results imply that ionic composition, rather than conductivity, plays a central role in determining the Faradaic efficiency of Fe(0) EC.

The E_A vs i curves for the carbonate, phosphate and nitrate electrolytes had similar shape to that of chloride and bromide but were uniformly offset by +2 to +4 V vs Ag/AgCl (Fig. 3d). The E_A vs i curves for the carbonate, phosphate and nitrate electrolytes overlap almost perfectly, which is consistent with the similarly low Faradaic efficiencies for these electrolytes. Interestingly, at $i > 3$ mA/cm^2, the E_A measurements for these electrolytes are identical to those of the sulfate electrolyte, which also had poor Faradaic efficiency in this i-range. The high E_A (> 1.4 V vs. Ag/AgCl) observed in the carbonate, phosphate and nitrate solutions at all i was accompanied by the formation of gas bubbles on the anode (Fig. S4) and poor Faradaic efficiency. In addition, dissolved O_2 measurements in the nitrate solution (Fig. S5)

revealed a rapid increase in dissolved O_2, with values reaching above the air saturated maximum of approximately 9 mg/L, which provides conclusive evidence for the anodic formation of O_2 in these three solutions.

3.2.3. Citrate and formate

The properties of the formate solution were most similar to those of the sulfate solution, with the Faradaic efficiency exhibiting a strong i-dependence (Fig. 3e). However, even at low i, the Faradaic efficiency in the formate solution was never as high as for sulfate. The Faradaic efficiency in the formate solution also decreased gradually with i, i.e. a transitional Faradaic efficiency near 0.5 was observed at $i = 1$ mA/cm^2. For the citrate solution, the Faradaic efficiency resembled that of the nitrate solution, with negligible electrochemical Fe(0) oxidation throughout the entire i-range. Furthermore, consistent with the nitrate solution, the surface of the Fe(0) anode after 10 electrochemical experiments in the citrate solution resembled that of a freshly polished Fe (0) anode (Fig. 4, Figs. S1 and S2), indicating surface passivation.

The E_A at the lowest i (highest Faradaic efficiency) in the formate solution was similar to that of chloride/bromide, but at $i > 1$ mA/cm^2, the E_A vs i curve followed that of nitrate. Similar to the results in the sulfate solution, the crossover i between high and low Faradaic efficiency in the formate solution coincided with an abrupt increase in E_A. For citrate, the position and shape of the E_A vs i curve resembled that of the nitrate solution, which is consistent with its poor Faradaic efficiency.

3.3. Impact of pH on the Faradaic efficiency and E_A

The influence of pH was examined in the sulfate and phosphate solutions because these ions affected the Faradaic efficiency differently in single anion systems (Fig. 3) and also have distinct pH dependent speciation, i.e. the dominant sulfate species remains as SO_4^{2-} above pH 3 (pK$_{a1}$ = −3, pK$_{a2}$ = 1.9), whereas phosphate deprotonates (pK$_{a1}$ = 2.1, pK$_{a2}$ = 7.2, pK$_{a3}$ = 12.7) [47]. For both sulfate and phosphate solutions, the Faradaic efficiency and E_A ($i = 1$ and 3 mA/cm^2) depended strongly on pH. At i-values of 1 and 3 mA/cm^2, the Faradaic efficiencies in the sulfate and phosphate solutions were above 1.0 at acidic pH (4.0 ± 0.5) and below 0.1 at basic pH (11.0 ± 0.5). Faradaic efficiencies above 1.0 for both acidic sulfate and phosphate
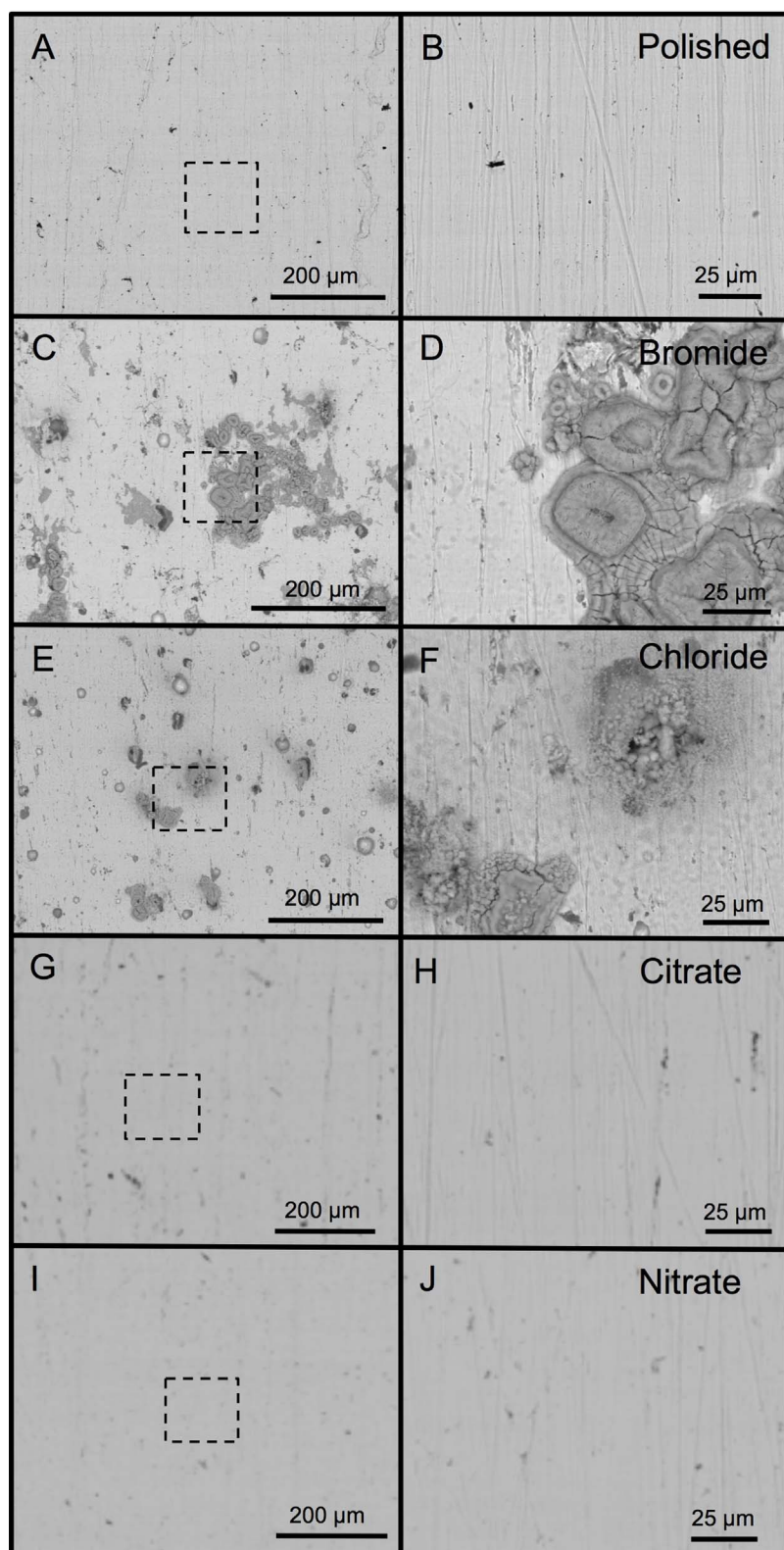
Fig. 4. Scanning electron micrographs of a polished Fe(0) anode (A and B), and Fe(0) anodes after 10 runs in various electrolyte solutions: bromide (C and D), chloride (E and F), citrate (G and H), nitrate (I and J). The panels on the right are magnified from the region in the dotted rectangles on the left.

solutions can be explained by chemical induced release of Fe, likely a result of proton promoted Fe(0) oxidation. The major difference between the impact of pH in the sulfate and phosphate solutions is the threshold pH and i at which the Faradaic efficiency changes from high to low. For phosphate, efficient electrochemical Fe(0) oxidation was only observed at acidic pH, whereas the Faradaic efficiency remained high at circumneutral pH in the sulfate solution at $i = 1$ mA/cm^2.

The same inverse relationship between Faradaic efficiency and E_A found in the single anion solutions was also observed in the sulfate and phosphate solutions at different pH values. For example, the lowest E_A for both solutions was observed at acidic pH, which showed the highest Faradaic efficiencies, whereas E_A was greater than 1.0 V vs Ag/AgCl for all samples with poor Faradaic efficiency. It is also noteworthy that decreasing solution pH from 7.5 ± 0.5 to 4.0 ± 0.5 decreased the

open circuit potential (i.e. the E_A in the absence of current) for both solutions from ~ -0.1 to -0.5 V vs Ag/AgCl.

3.4. Faradaic efficiency in chloride containing, binary anion solutions

In Section 3.2, we found that the behavior of the chloride solution contrasted that of the nitrate and carbonate solutions with respect to Faradaic efficiency and E_A. Therefore, to evaluate the relative impact of ubiquitous ions that facilitate or prevent electrochemical Fe(0) oxidation, we performed EC experiments ($i = 1$ mA/cm^2) in binary anion solutions with a wide range of nitrate to chloride or carbonate to chloride molar ratios ($[NO_3^-]/[Cl^-]$ or $[HCO_3^-]/[Cl^-]$ = 0.1–1000 mol/mol; $[NO_3^-]$ and $[HCO_3^-]$ = 10 mM for $[NO_3^-]/[Cl^-]$ and $[HCO_3^-]/[Cl^-] \geq 1$).

At $[NO_3^-]/[Cl^-]$ molar ratios below 20, the nitrate and chloride binary anion solution behaved similarly to the chloride solution, with high Faradaic efficiencies and $E_A < 0.5$ V vs Ag/AgCl. The persistence of efficient electrochemical Fe(0) oxidation and low E_A at $[NO_3^-]/[Cl^-]$ ratios near 1.0 indicates that the presence of chloride outweighs the detrimental impacts of nitrate on an equimolar basis. However, at $[NO_3^-]/[Cl^-]$ ratios above 30, the Faradaic efficiency decreased and the E_A increased, leading to a solution with properties akin to the nitrate single anion system. These abrupt changes in Faradaic efficiency and E_A suggest that a narrow range of $[NO_3^-]/[Cl^-]$ ratios near 20 to 30 separate the electrochemical domains of Fe(0) oxidation and O_2 evolution in the Fe(0) EC system.

The relationship between Faradaic efficiency and E_A with increasing $[HCO_3^-]/[Cl^-]$ was similar as that for the nitrate and chloride system, but the transition from high to low Faradaic efficiency occurred at a greater $[HCO_3^-]/[Cl^-]$ ratio. Whereas the drop in Faradaic efficiency and spike in E_A occurred above $[NO_3^-]/[Cl^-]$ ratios of 20, the critical $[HCO_3^-]/[Cl^-]$ ratio was 100. This indicates that carbonate solutions require a lower chloride content to ensure efficient electrochemical Fe(0) oxidation than nitrate solutions.

3.5. Faradaic efficiency as a function of i in synthetic groundwaters

In Fig. 7, the Faradaic efficiency and E_A are plotted as a function of i for synthetic Bangladesh groundwater (SBGW) and for two synthetic nitrate contaminated groundwaters (NO$_3$-GW 1 and NO$_3$-GW 2). The ionic composition and pH of these synthetic groundwaters, which cover a range of potential source waters for Fe(0) EC treatment, are summarized in Table 2. High Faradaic efficiency in the SBGW solution was observed for all i, which is consistent with its high chloride concentration and low $[HCO_3^-]/[Cl^-]$ and $[NO_3^-]/[Cl^-]$ ratios. Coinciding with the high Faradaic efficiency, the E_A vs i curve for the SBGW solution also matched the shape and position of that for the chloride single anion solution. By contrast, the poor Faradaic efficiency and high E_A for the NO$_3$-GW 1 solution resembled those of the nitrate solution, which agrees with the $[NO_3^-]/[Cl^-]$ molar ratio above 30 for this solution. Despite the 15 fold increase in conductivity for the NO$_3$-GW 1 solution relative to the nitrate solution and the presence of 0.5 mM chloride, the NO$_3$-GW 1 solution still displayed poor Faradaic efficiency. This result points to the key role of the $[NO_3^-]/[Cl^-]$ molar ratio in determining the Faradaic efficiency, rather than the conductivity or absolute chloride concentration.

For the NO$_3$-GW 2 solution, the Faradaic efficiency was greater than 0.9 for $i \leq 10$ mA/cm^2 but dropped abruptly to below 0.1 at $i > 20$ mA/cm^2. Given the moderate $[NO_3^-]/[Cl^-]$ ratio of ~18 mol/mol for this solution, this result suggests that the $[NO_3^-]/[Cl^-]$ ratio dividing the domains of Fe(0) oxidation and O_2 evolution also depends on i. Furthermore, although acidic pH improved the Faradaic efficiency in sulfate and phosphate solutions (Section 3.3), the results in the NO$_3$-GW 2 matrix indicate that high i can still promote poor Faradaic efficiency in acidic solutions. The E_A vs i curve for the NO$_3$-GW 2 solution increased sharply at the i-value for which the Faradaic efficiency

decreased, which is similar to the E_A vs i curve for sulfate. Despite having a region of i where Faradaic efficiency was poor, the E_A vs i curve for the NO$_3$-GW 2 solution was positioned ~0.5 V vs Ag/AgCl lower than that of the chloride solution. We attribute this difference in the position of the E_A vs i curve for the NO$_3$-GW 2 matrix to its acidic pH, leading to a lower open circuit potential (-0.6 V vs Ag/AgCl) relative to the single anion solutions (-0.2 V vs Ag/AgCl). This was also observed in the acidic sulfate and phosphate solutions.

4. Discussion

4.1. Factors affecting the Faradaic efficiency

4.1.1. Ionic composition

For the majority of single anion solutions and synthetic groundwater matrices, the Faradaic efficiency was largely independent of i. Rather, the type of anion in the solution played a more critical role in governing the Faradaic efficiency and E_A, and thus the potential for electrode passivation. For example, regardless of i, Faradaic efficiency was high in the chloride and bromide solutions, whereas it was minimal in nitrate and citrate solutions. Modifications of the Fe(0) anode surface mirrored these trends in Faradaic efficiency, with the chloride and bromide solutions producing macroscopic surface layers of oxidized Fe and the nitrate and citrate solutions yielding passivated Fe(0) anode surfaces that resembled cleaned electrodes (Fig. 4, Figs. S1 and S2). Although previous EC studies have identified conductivity as a key operational parameter [7,31,48], our results demonstrate substantial differences among solutions with identical conductivity, which reveals the critical importance of the ion composition.

Comparing the Faradaic efficiency and E_A measurements as a function of i for all solutions in Fig. 3 (Section 3.2), it is possible to rank the anions in the following order of negative influence on Fe (0) EC performance: chloride $\leq$ bromide $<$ sulfate $<$ formate $<$ carbonate $\leq$ phosphate $\leq$ citrate $\leq$ nitrate. With the exception of nitrate, this sequence of anions generally follows the same order of increasing stability constants with Fe(II) or Fe(III) (Table S1). For example, chloride and bromide do not form strong complexes with Fe(II/III), whereas phosphate and citrate have a high affinity for Fe (II/III) [49,50]. A similar anion sequence has been observed in previous studies investigating the reactivity of Fe(0) metal toward contaminant reduction, which reported that chloride enhanced electron transfer, whereas the sorption of phosphate and citrate diminished the redox activity of Fe(0) metal by blocking reactive sites [32,33]. Therefore, based on this connection between detriment to Faradaic efficiency and the Fe(II/III) stability constants, the effect of single anions can be explained by the bonding of high affinity anions (e.g. phosphate, citrate) to oxidized Fe at the electrode surface, resulting in a thin, but impermeable passivating film that prevents the release of Fe(II/III) to solution. Although a molecular-scale investigation of the surface layers formed on the electrodes having poor Faradaic efficiency is beyond the scope of our work, the formation of a nanoscale passivating film is consistent with the absence of corrosion spots on the anodes used in the citrate experiments and is supported by previous studies reporting the formation of a phosphate-bearing layer that inhibits the corrosion of Fe and stainless steel in phosphate solutions [51,52].

The exception to the trends in anion sequence is nitrate, which inhibited Fe(0) oxidation but does not readily complex with Fe(II/III). However, the mechanism by which nitrate decreases the Faradaic efficiency is expected to be different than for anions with a high affinity for Fe (II/III). Rather than complexing with Fe(II/III) at the Fe(0) surface, nitrate is known to oxidize Fe(0) metal, producing a thin, Fe (oxyhydr)oxide passive film that inhibits ion diffusion [32]. Despite the different inhibition mechanisms expected for nitrate and high affinity anions, both mechanisms are expected to lead to nanoscale passivating films on the Fe(0) anode surface, which are imperceptible with SEM [53,54].
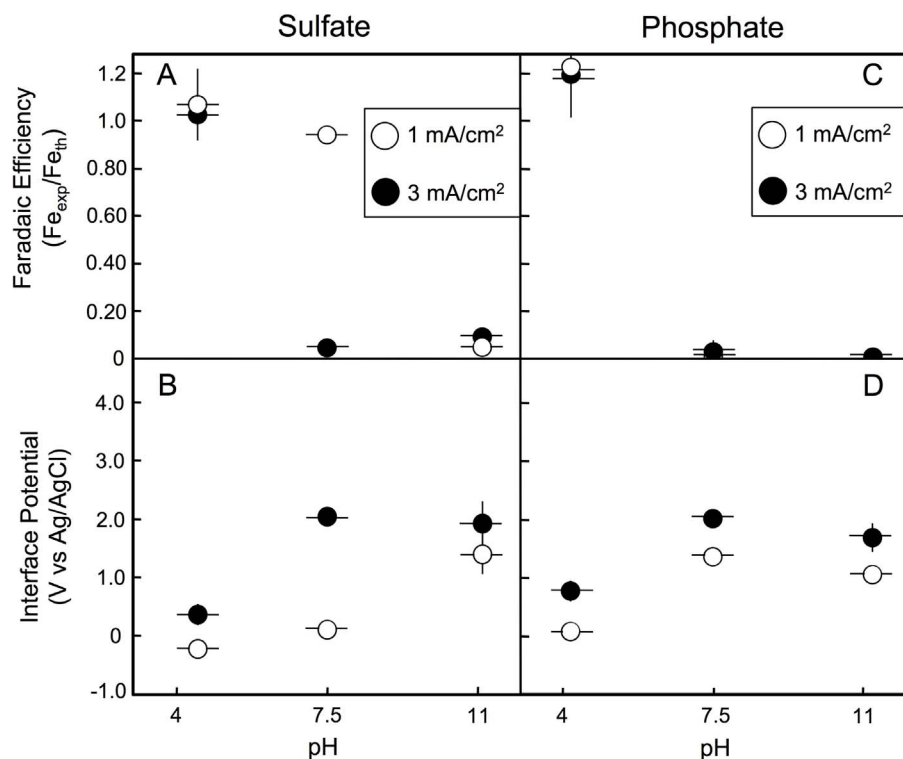
Fig. 5. Influence of solution pH on the Faradaic efficiency and anodic interface potential from Fe(0) EC experiments performed at current densities of 1 (empty circles) and 3 mA/cm² (filled circles) in 5 mM sulfate (A and B) and 5 mM phosphate (C and D) solutions. Error bars indicate the maximum drift in pH observed during experiments. The open circuit potential of the low pH samples for both solutions was −0.6 to −0.4 V vs Ag/AgCl, whereas at circumneutral pH and above, the open circuit potential was −0.2 to −0.1 V vs Ag/AgCl.

4.1.2. Range of i

For the single anion sulfate and formate solutions and the synthetic NO_3-GW 2 matrix, the i-range influenced the domains of Fe(0) oxidation and O_2 evolution. Importantly, the three solutions also displayed intermediate properties with respect to ionic composition and pH. For example, the stability constants of sulfate and formate for Fe(II/III) lie between those of chloride/bromide and phosphate/citrate [50]. In addition, the $[NO_3^-]/[Cl^-]$ ratio for the NO_3-GW 2 solution (18 mol/mol) occurs near the threshold ratio (20–30 mol/mol) that separates Fe(0) oxidation and O_2 evolution (Fig. 5). Although i was less important for end member solutions of the anion sequence described in Section 4.1.1, this parameter played an important secondary role for solutions with intermediate compositions.

We attribute the impact of i on the anodic reaction and potential for electrode passivation to the Butler-Volmer relationship, given in Eq. (2), which shows that an increase in i leads to an increase in E_A. Because an increase in E_A can promote anodic reactions with high E^0 (Fig. 1a), an increase in i can lead to the oxidation of H_2O or other solutes instead of Fe(0), which would decrease the Faradaic efficiency. Consistent with this relationship, we observed a nonlinear jump in E_A when the dominant anodic reaction switched from Fe(0) oxidation to O_2 evolution (Fig. 3) for solutions in which the Faradaic efficiency depended on i (e.g. sulfate). For the sulfate solution, the magnitude of this jump in E_A (≈ 2 V vs Ag/AgCl) was the exact value separating the E_A vs i curves for Fe(0) oxidation (chloride/bromide) and O_2 evolution (citrate/nitrate). Therefore, we conclude that the measurements of the position of the E_A vs i curve can be a useful and low cost indicator of the anodic reaction occurring during Fe(0) EC.

4.1.3. Solution pH

For both the sulfate and phosphate solutions, pH influenced the Faradaic efficiency considerably, with efficient Fe(0) oxidation occurring only at low pH. Considering that phosphate is a detrimental end member species in the anion sequence (Section 4.1.1), the high Faradaic efficiency observed in the phosphate solution at low pH suggests that pH effects can overcome the negative impact caused by high affinity anions, particularly at low i. The pH dependence of the Faradaic

efficiency observed in our study can be explained by a number of contemporaneous processes. First, as pH increases, E^0 for the H_2O/O_2 redox couple decreases [50], leading to a narrower field of H_2O stability and increased likelihood of O_2 evolution for a given E_A. Second, increasing pH leads to orders of magnitude faster rates for Fe(II) oxidation by O_2 [55] as well as decreased Fe(III) solubility (see Supplementary material for speciation calculations and Fig. S5 for Fe(III) saturation indices). Both of these processes, which are applicable in all solutions regardless of ion composition, are expected to promote the formation of Fe(III) (oxyhydr)oxide passivating films that inhibit electron transfer across the anode and Fe(II/III) release. Finally, for the phosphate electrolyte, the solubility of Fe(II) in the presence of phosphate depends strongly on pH. For example, as pH increases from 4 to 7, the saturation index of vivianite ($Fe_3(PO_4)_2 \cdot 8H_2O$) increases ~10 orders of magnitude (−2.9 to 7.4, Fig. S6), leading to conditions that favor the formation of anodic surface layers that inhibit Fe(II) release. These pH dependent changes in solid phase solubility in the phosphate solution, which do not occur to the same extent in the sulfate solution (Fig. S6), explain the stronger impact of pH in the presence of phosphate relative to sulfate (Fig. 6).

4.2. Implications for EC treatment in the field

4.2.1. Field treatment recommendations

Effective treatment of contaminated waters by Fe(0) EC relies on the production and transport of Fe(II) from the Fe(0) anode surface to the bulk solution. For example, Cr(VI) is removed in EC systems by reaction with EC generated Fe(II), to form insoluble Cr(III) [6,7], whereas As(III) is removed by oxidation to As(V) by Fenton type intermediates and sorption to EC generated Fe(III) precipitates [35,56]. Therefore, regardless of the contaminant removal mechanism, a critical loss of treatment efficiency occurs when the applied current drives O_2 evolution at the expense of Fe(0) oxidation. In addition, as shown in this work, a drop in Faradaic efficiency is accompanied by a spike in E_A, which is consistent with electrode passivation. This increases the total EC cell voltage and can result in higher power consumption during EC treatment. Therefore, EC system effectiveness in the field relies on
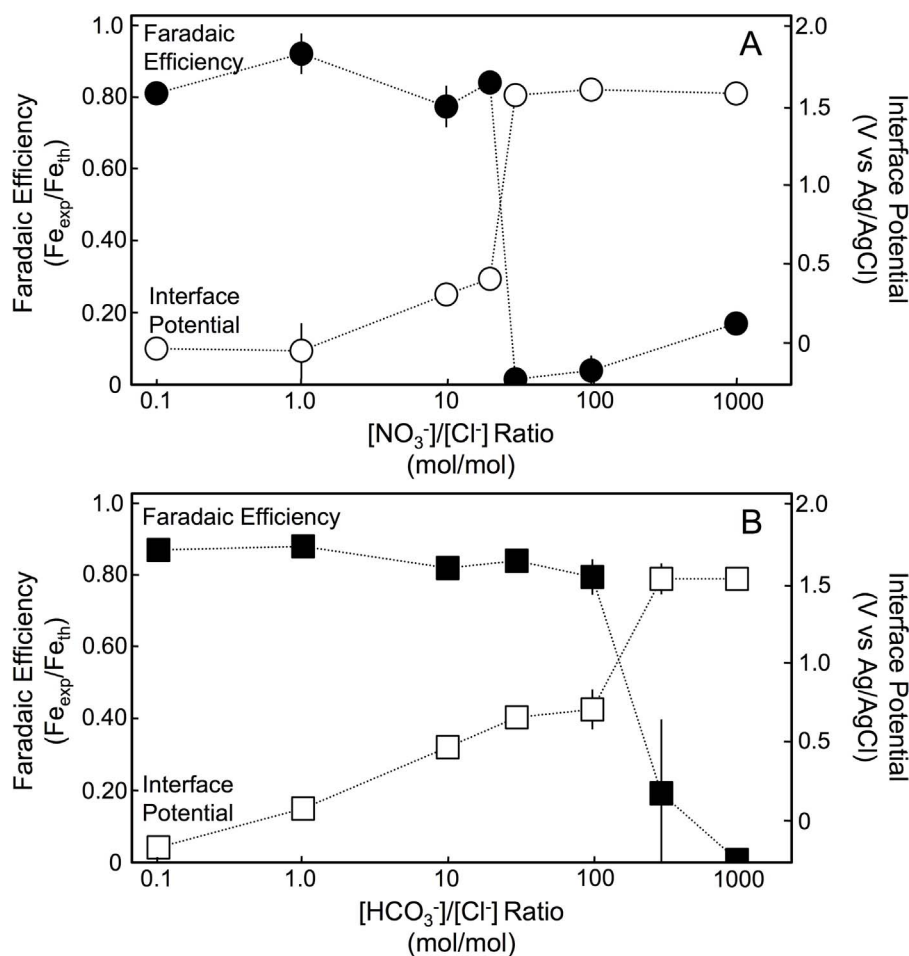
Fig. 6. Influence of the (A) $[NO_3^-]/[Cl^-]$ and (B) $[HCO_3^-]/$ $[Cl^-]$ molar ratios on the Faradaic efficiency and E_A for Fe(0) EC experiments performed at $i = 1$ mA/cm². Filled symbols represent Faradaic efficiency; empty symbols indicate E_A.
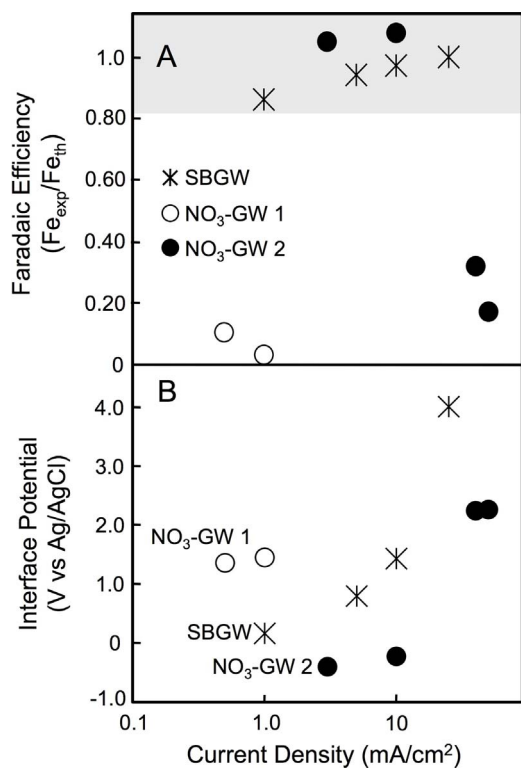

Fig. 7. Faradaic efficiency (A) and anodic interface potential (B) as a function of i for three synthetic groundwaters (composition presented in Table 2).

avoiding poor Faradaic efficiency.

Based on our results, the i-range can impact the Faradaic efficiency for specific solution compositions, with efficient Fe(0) oxidation favored at $i < 5$ mA/cm², which is similar to the i-range used in previous Fe(0) EC field experiments [3]. However, although i should not be ignored in field treatment, our results indicate that the solution composition is the dominant parameter governing the Faradaic efficiency. Source waters with low chloride levels, alkaline pH and high concentrations of nitrate, carbonate and other high affinity oxyanions can be a barrier to high Faradaic efficiency. Treatment influents with such solution chemistry can be encountered in nitrate contaminated groundwater systems, including those impacted by agricultural runoff [57], sewage [58], and radionuclide enrichment activities [37,42,44]. Furthermore, chloride concentrations in groundwaters contaminated by geogenic arsenic can be low and $[HCO_3^-]/[Cl^-]$ ratios above the critical ratio of 100 mol/mol (Fig. 6) are not uncommon in regions targeted for Fe(0) EC treatment in South Asia (e.g. Table 7.1 in the British Geologic Survey analysis of Bangladeshi groundwater [39]).

Although decreasing pH to near 4 can negate some of the impacts of ion composition, adjusting pH at field treatment scale is impractical for several reasons, e.g. hazardous and costly chemicals, pH readjustment of treatment effluent, skilled labor requirement. Instead, our results indicate that an influent composition favoring O_2 evolution can be overcome easily and at low cost by simple additions of small quantities of NaCl (table salt) prior to electrolysis. Although the importance of halide ions to Fe(0) EC performance has been suggested previously [25,31,48], our results have uncovered distinct $[NO_3^-]/[Cl^-]$ and $[HCO_3^-]/[Cl^-]$ molar ratios that separate the Fe(0) oxidation and O_2 evolution domains (Fig. 6). Based on this ratio, the addition of 1 mM NaCl can overcome nitrate and carbonate concentrations up to 20 and

100 mM, respectively. This result suggests that a single purchase of 10 kg NaCl can provide enough chloride to treat over 150 m^3 of groundwater containing moderate to high nitrate or carbonate levels. Previous analyses of fully operational Fe(0) EC systems (10,000 L/d capacity) have estimated total costs to be < $1.50/m^3 of treated water [3], which includes consumable costs ($0.44/m^3, iron plates, electricity, additional chemicals) and system fabrication and labor costs ($1.04/m^3), but excludes sludge disposal (estimated < 5% of total costs). Therefore, assuming a conservative price of table salt ($10/ 10 kg), the proposed addition of small quantities of NaCl to ensure high Faradaic efficiency would increase these estimated costs < 5%. Although this option adds a pretreatment step, it is very simple and does not require hazardous chemicals or major supply chain infrastructure and would render the electrolyte solution suitable for a wide range of i. In addition, our results indicate that measurement of E_A, which does not require expensive equipment, and comparison of this value with i can inform system operators when NaCl treatment is required.

4.2.2. Insights into field treatment performance over time

Several previous Fe(0) EC field studies have reported a drop in system performance over extended operating times (weeks to months) and cycles of electrode polarization, i.e. periods of operation (wet) and storage (dry) [45,59]. One previously proposed explanation for this decreased field performance is a drop in Faradaic efficiency resulting from O$_2$ evolution after many cycles of operation. However, extended EC field trials typically contain few systematic measurements of key parameters over time, i.e. no regular measurements of E_A or Fe in suspension [3]. As a consequence, explanations of the efficiency drop observed during field treatment remain speculative.

We observed a subtle decrease in the Faradaic efficiency on single run time scales (Fig. 2), which was reproduced in both the sulfate and chloride solutions. Over the 10 runs required to produce anode samples for SEM imaging, a decrease in the Faradaic efficiency was also observed (Fig. S7). These drops in Faradaic efficiency over a single run (Fig. 2) or multiple runs (Fig. S7) did not coincide with an offset in E_A indicative of O$_2$ evolution (or Fe(III) production). Although Fe(0) EC field systems differ in size and treatment time relative to our experimental setup [1,3,59], the absence of an increase in E_A over several days (10 runs) in this work suggests that O$_2$ evolution after extended treatment cycles in the field is not the primary cause of decreased system performance. This conclusion is consistent with the relatively low i (~1 mA/cm^2) used in previous Fe(0) EC field trials [3]. Rather, in light of the build up of anodic surface layers in the chloride/bromide solution (Fig. 4, Figs. S1 and S2), our results support the hypothesis that field treatment performance decreases over time because EC generated Fe(II) is trapped at the anode by macroscopic Fe (oxyhydr)oxide surface layers (e.g. magnetite, goethite) formed on the electrode after extended operation [45].

5. Conclusions

The ionic composition and pH of the electrolyte solution largely determined the Faradaic efficiency of Fe(0) EC, with changes in i influencing the domains of Fe(II) production and O$_2$ evolution only in certain electrolyte solutions (e.g. sulfate and formate). By ranking single anion solutions according to their detriment to Faradaic efficiency (chloride ≤ bromide < sulfate < formate < carbonate ≤ phosphate ≤ citrate ≤ nitrate), we elucidated a useful relationship between the propensity of ions to form strong complexes with Fe(II,III) and low Faradaic efficiency. The exception to this trend is nitrate, which is expected to interact with the Fe(0) anode differently [32]. Based on this relationship, we expect that solutions containing ions with strong affinity for Fe(II/III), such as silicate, would favor O$_2$ evolution, whereas solutions containing ions such as iodide and fluoride, which have a weaker affinity for Fe (II,III) [50], promote Fe(0) oxidation. In chloride containing,

binary anion solutions, we found the domains of Fe(0) oxidation and O$_2$ evolution ($i = 1$ mA/cm^2) were separated by discreet [NO$_3^-$]/[Cl$^-$] and [HCO$_3^-$]/[Cl$^-$] molar ratios, which were confirmed in synthetic groundwater solutions. This result indicates that a simple amendment of NaCl to source waters with compositions that favor O$_2$ evolution (e.g. sites of nitrate pollution or arsenic contaminated groundwater with low chloride content) can ensure high Faradaic efficiency, which is critical to optimize the performance of Fe(0) EC systems in the field.

The E_A vs i curves for the chloride and bromide solutions overlapped and reached E_A far greater than the E^0 of H$_2$O/O$_2$, Cl$^-$/Cl$_2$ and Br$^-$/Br$_2$ couples, but high Faradaic efficiency was still observed in these solutions. This conclusion demonstrates that significant anodic Cl$_2$ and Br$_2$ formation is unlikely to occur during Fe(0) EC even at extreme E_A (and i), although their formation has been reported for different electrode materials (e.g. boron-doped diamond or Al(0) electrodes) [60,61]. Finally, the E_A vs i curves for the citrate and nitrate solutions, which exhibited poor Faradaic efficiency, also overlapped and were situated 2–4 V vs Ag/AgCl above that of the chloride/bromide solutions. Comparison between the E_A vs i curves of both high and low Faradaic efficiency solutions showed that the E_A vs i curve, rather than the E_A alone, is necessary to identify the primary reaction occurring on the Fe (0) anode. This information can be used to accurately determine in real time if Fe(0) EC systems are operating at high Faradaic efficiency using only simple, low cost, and chemical-free field measurements of E_A with knowledge of i.

Appendix A. Supplementary data

Supplementary data associated with this article can be found, in the online version, at http://dx.doi.org/10.1016/j.jece.2017.09.008.

References

[1] P. Holt, G. Barton, C. Mitchell, Chemosphere 59 (3) (2005) 355–367, http://dx.doi.org/10.1016/j.chemosphere.2004.10.023.
[2] S.E. Amrose, Z. Burt, I. Ray, Annu. Rev. Environ. Resour. 40 (9) (2015) 203–231, http://dx.doi.org/10.1146/annurev-environ-031411-091819.
[3] S.E. Amrose, S.R.S. Bandaru, C. Delaire, C.M. van Genuchten, A. Dutta, A. DebSarkar, C. Orr, J. Roy, A. Das, A.J. Gadgil, Sci. Total Environ. 488–489 (2014) 539–546.
[4] D. Lakshmanan, D.A. Clifford, G. Samanta, Environ. Sci. Technol. 43 (10) (2009) 3853–3859, http://dx.doi.org/10.1021/Es8036669.
[5] D. Ghernaout, Desalin. Water Treat. 51 (40–42) (2013) 7536–7554, http://dx.doi.org/10.1080/19443994.2013.792520.
[6] G. Mouedhen, M. Feki, M. De Petris-Wery, H. Ayedi, J. Hazard. Mater. 168 (2–3) (2009) 983–991, http://dx.doi.org/10.1016/j.jhazmat.2009.02.117.
[7] T. Olmez, J. Hazard. Mater. 162 (2–3) (2009) 1371–1378, http://dx.doi.org/10.1016/j.jhazmat.2008.06.017.
[8] Z. Yang, H. Xu, G. Zeng, Y. Luo, X. Yang, J. Huang, L. Wang, P. Song, Electrochim. Acta 153 (2015) 149–158, http://dx.doi.org/10.1016/j.electacta.2014.11.183.
[9] K. Cheballah, A. Sahmoune, K. Messaoudi, N. Drouiche, H. Lounici, Chem. Eng. Process. 96 (2015) 94–99, http://dx.doi.org/10.1016/j.cep.2015.08.007.
[10] S.J. Hug, O. Leupin, Environ. Sci. Technol. 37 (12) (2003) 2734–2742, http://dx.doi.org/10.1021/Es026208x.
[11] C. van Genuchten, J. Pena, Environ. Sci. Technol. 51 (5) (2017) 2982–2991, http://dx.doi.org/10.1021/acs.est.6b05584.
[12] P.R. Kumar, S. Chaudhari, K.C. Khilar, S.P. Mahajan, Chemosphere 55 (9) (2004) 1245–1252, http://dx.doi.org/10.1016/j.chemosphere.2003.12.025.
[13] P. Song, Z. Yang, G. Zeng, X. Yang, H. Xu, L. Wang, R. Xu, W. Xiong, K. Ahmad, Chem. Eng. J. 317 (2017) 707–725.
[14] C. Escobar, C. Soto-Salazar, M.I. Toral, J. Environ. Manage. 81 (4) (2006) 384–391, http://dx.doi.org/10.1016/j.jenvman.2005.11.012.

[15] C.X.-H. Su, L.W. Low, T.T. Teng, Y.S. Wong, J. Environ. Chem. Eng. 4 (2016) 3618–3631.
[16] W. Lemlikchi, S. Khaldi, M. Mecherri, H. Lounici, N. Drouiche, Sep. Sci. Technol. 47 (11) (2012) 1682–1688, http://dx.doi.org/10.1080/01496395.2011.647374.
[17] B. Yang, Y. Han, G. Yu, Q. Zhuo, S. Deng, J. Wu, P. Zhang, Chem. Eng. J. 303 (2016) 384–390, http://dx.doi.org/10.1016/j.cej.2016.06.011.
[18] C. Delaire, C.M. van Genuchten, K.L. Nelson, S.E. Amrose, A.J. Gadgil, Environ. Sci. Technol. 49 (16) (2015) 9945–9953, http://dx.doi.org/10.1021/acs.est.5b01696.
[19] S. Chellam, M. Sari, J. Hazard. Mater. 304 (5) (2016) 490–501, http://dx.doi.org/10.1016/j.jhazmat.2015.10.054.
[20] D. Manenti, A. Modenes, P. Soares, F. Espinoza-Quinones, R. Boaventura, R. Bergamasco, V. Vilar, Chem. Eng. J. 252 (2014) 120–130, http://dx.doi.org/10.1016/j.cej.2014.04.096.
[21] M. Sari, S. Chellam, J. Colloid Interface Sci. 458 (15) (2015) 103–111, http://dx.doi.org/10.1016/j.jcis.2015.07.035.
[22] C.M. van Genuchten, J. Pena, S.E. Amrose, A.J. Gadgil, Geochim. Cosmochim. Acta 127 (2014) 285–304.
[23] C.M. van Genuchten, A.J. Gadgil, J. Pena, Environ. Sci. Technol. 48 (20) (2014) 11828–11836.
[24] K. Dubrawski, C. Du, M. Mohseni, Electrochim. Acta 129 (2014) 187–195, http://dx.doi.org/10.1016/j.electacta.2014.02.089.
[25] G. Mouedhen, M. Feki, M. Wery, H. Ayedi, J. Hazard. Mater. 150 (1) (2008) 124–135, http://dx.doi.org/10.1016/j.jhazmat.2007.04.090.
[26] J. Hakizimana, B. Gourich, M. Chafi, Y. Stiriba, C. Vial, P. Drogui, J. Naja, Desalination 404 (2017) 1–21, http://dx.doi.org/10.1016/j.desal.2016.10.011.
[27] J. Lu, Z. Wang, X. Ma, Q. Tang, Y. Li, Chem. Eng. Sci. 165 (2017) 165–176.
[28] A.J. Bard, L.R. Faulkner, Electrochemical Methods: Fundamentals and Applications, 2nd ed., Wiley, New York, 2001.
[29] K.L. Dubrawski, C.M. van Genuchten, C. Delaire, S.E. Amrose, A.J. Gadgil, M. Mohseni, Environ. Sci. Technol. 49 (17) (2015) 2171–2179, http://dx.doi.org/10.1021/es505059d.
[30] I. Heidmann, W. Calmano, Sep. Purif. Technol. 61 (1) (2008) 15–21, http://dx.doi.org/10.1016/j.seppur.2007.09.011.
[31] M. Arroyo, V. Perez-Herranz, M. Montanes, J. Garcia-Anton, J. Guinon, J. Hazard. Mater. 169 (1–3) (2009) 1127–1133, http://dx.doi.org/10.1016/j.jhazmat.2009.04.089.
[32] B. Reinsch, B. Forsberg, R. Penn, C. Kim, G. Lowry, Environ. Sci. Technol. 44 (9) (2010) 3455–3461, http://dx.doi.org/10.1021/es902924h.
[33] C. Su, R. Puls, Environ. Sci. Technol. 38 (9) (2004) 2715–2720, http://dx.doi.org/10.1021/es034650p.
[34] C. Noubactep, A. Schoner, J. Hazard. Mater. 175 (1–3) (2010) 1075–1080, http://dx.doi.org/10.1016/j.jhazmat.2009.09.152.
[35] C. van Genuchten, S. Addy, J. Pena, A. Gadgil, Environ. Sci. Technol. 46 (2) (2012) 986–994, http://dx.doi.org/10.1021/es201913a.
[36] W. Wan, T. Pepping, T. Banerji, S. Chaudhari, D. Giammar, Water Res. 45 (1) (2011) 384–392, http://dx.doi.org/10.1016/j.watres.2010.08.016.
[37] USEPA, CURE Electrocoagulation Technology, Innovative Technology Evaluation Report, National Risk Management Research, Laboratory Office of Research and Development, 1998.
[38] N.K. Shammas, M.-F. Pouet, A. Grasmick, L.K. Wang (Ed.), Handbook of Environmental Engineering, 2010.
[39] BGS, Arsenic Contamination of Groundwater in Bangladesh, British Geological Survey, 2001.
[40] A. Abdelouas, Y. Lu, W. Lutze, H. Nuttall, J. Contam. Hydrol. 35 (1–3) (1998) 217–233, http://dx.doi.org/10.1016/S0169-7722(98)00134-X.
[41] J. Istok, J. Senko, L. Krumholz, D. Watson, M. Bogle, A. Peacock, Y. Chang, D. White, Environ. Sci. Technol. 38 (2) (2004) 468–475, http://dx.doi.org/10.1021/es034639p.
[42] S. Kamp, S. Morrison, Ground Water Monit. Rem. 34 (1) (2014) 68–78, http://dx.doi.org/10.1111/gwmr.12042.
[43] W. Wu, J. Carley, M. Fienen, T. Mehlhorn, K. Lowe, J. Nyman, J. Luo, M. Gentile, R. Rajan, D. Wagner, R. Hickey, B. Gu, D. Watson, O. Cirpka, P. Kitanidis, P. Jardine, C. Criddle, Environ. Sci. Technol. 40 (12) (2006) 3978–3985, http://dx.doi.org/10.1021/es051954y.
[44] T. Yan, M. Fields, L. Wu, Y. Zu, J. Tiedje, J. Zhou, Environ. Microbiol. 5 (1) (2003) 13–24, http://dx.doi.org/10.1046/j.1462-2920.2003.00393.x.
[45] C.M. van Genuchten, S.R.S. Bandaru, E. Surorova, S.E. Amrose, A.J. Gadgil, J. Pena, Chemosphere 153 (2016) 270–279.
[46] B. Reinsch, B. Forsberg, R. Penn, C. Kim, G. Lowry, Environ. Sci. Technol. 44 (9) (2010) 3455–3461, http://dx.doi.org/10.1021/es902924h.
[47] J.E. Ricci, J. Am. Chem. Soc. 70 (1) (1948) 109–113, http://dx.doi.org/10.1021/ja01181a031.
[48] G. Chen, Sep. Purif. Technol. 38 (1) (2004) 11–41, http://dx.doi.org/10.1016/j.seppur.2003.10.006.
[49] J.P. Gustafsson, Visual Minteq v. 3.0, Vol. 2013 (in Series), KTH, Stockholm, Sweden, 2013.
[50] M.M. Benjamin, Water Chemistry, McGraw-Hill Series in Water Resources and Environmental Engineering, McGraw-Hill, Boston, 2002.
[51] A. Guenbour, J. Faucheu, A. Benbachir, Corrosion 44 (4) (1988) 214–221.
[52] M. Bojinov, I. Betova, G. Fabricius, T. Laitinen, R. Raicheff, J. Electroanal. Chem. 475 (1) (1999) 58–65, http://dx.doi.org/10.1016/S0022-0728(99)00343-5.
[53] C. Shih, C. Shih, Y. Su, L. Su, M. Chang, S. Lin, Corros. Sci. 46 (2) (2004) 427–441, http://dx.doi.org/10.1016/S0010-938X(03)00148-3.
[54] C. Olsson, D. Landolt, Electrochim. Acta 48 (9) (2003) 1093–1104, http://dx.doi.org/10.1016/S0013-4686(02)00841-1.
[55] W. Stumm, G. Lee, Ind. Eng. Chem. 53 (2) (1961) 143–146, http://dx.doi.org/10.1021/ie50614a030.
[56] L. Li, C.M. van Genuchten, S.E.A. Addy, J. Yao, N. Gao, A.J. Gadgil, Environ. Sci. Technol. 46 (21) (2012) 12038–12045.
[57] K. Burow, B. Jurgens, K. Belitz, N. Dubrovsky, Environ. Earth Sci. 69 (8) (2013) 2609–2621, http://dx.doi.org/10.1007/s12665-012-2082-4.
[58] S. Suthar, P. Bishnoi, S. Singh, P. Mutiyar, A. Nema, N. Patil, J. Hazard. Mater. 171 (1–3) (2009) 189–199, http://dx.doi.org/10.1016/j.jhazmat.2009.05.111.
[59] T. Timmes, H. Kim, B. Dempsey, Desalination 250 (1) (2010) 6–13, http://dx.doi.org/10.1016/j.desal.2009.03.021.
[60] S. Ferro, A. De Battisti, I. Duo, C. Comninellis, W. Haenni, A. Perret, J. Electrochem. Soc. 147 (7) (2000) 2614–2619, http://dx.doi.org/10.1149/1.1393578.
[61] S. Gao, M. Du, J. Tian, J. Yang, J. Yang, F. Ma, J. Nan, J. Hazard. Mater. 182 (1–3) (2010) 827–834, http://dx.doi.org/10.1016/j.jhazmat.2010.06.114.
[62] R. Griffin, J. Jurinak, Soil Sci. 116 (1) (1973) 26–30.